UNIVERSITY OF CALIFORNIA SAN DIEGO

Prototyping a Power Take-off for the Wirewalker Wave-powered Profiling Vehicle

A Thesis submitted in partial satisfaction of the requirements
for the degree Master of Science

in

Mechanical Engineering

by

Thomas Kelly

Committee in charge:

Professor Drew Lucas, Chair
Professor Jennifer Mackinnon
Professor Geno Pawlak

2023

The Thesis of Thomas Kelly is approved, and it is acceptable in quality and form for publication on microfilm and electronically.

University of California San Diego

2023

TABLE OF CONTENTS

LIST OF FIGURES & TABLES

APPENDIX

ABSTRACT OF THE THESIS

Prototyping a Power Take-off for the Wirewalker Wave-powered Profiling Vehicle

by

Thomas Kelly

Master of Science in Mechanical Engineering

University of California San Diego, 2023

Professor Drew Lucas, Chair

Wirewalker vertical profilers have become a common tool for oceanographic research, but the energy required by onboard sensors sets up a maximum horizon for deployment before ongoing recovery and re-deployment becomes impractical and expensive. Given that the Wirewalker mechanically harnesses energy from ocean surface waves to drive propulsion, a natural next step for the Wirewalker system is using ocean wave energy to power the onboard sensors.

This paper documents the design process for a 3-wheel power take-off system that merges the submersible motor-generator (Livewire), designed by Dr. Michael Goldin and Prof. Drew Lucas,

within a Wirewalker frame. The as-tested “omega-configuration” power take-off relies on the grip of a single wheel on the mooring wire to both cam in one direction (allowing profiling mechanically driven by the surface waves, as in the Wirewalker) and also efficiently generate power. Basic profiling dynamics and experimental results inspired a design that pushes the generator wheel between two sheaves, while allowing it to hinge up and down to passively increase grip on the wire as the power available in any particular wave cycle increases. Tests in the Scripps pool generated a peak power of 1 Watt, with a time average 0.1 Watts. However, this result was likely related to slipping and frictional losses, which also was observed to inhibit 1-way camming motion. Future iterations of the 3-wheel power take-off should wrap the wire further around the wheel, investigate wheel surfaces with a higher coefficient of friction, and reduce internal friction losses with better constrained sheaves.

CHAPTER 1: Introduction

1.1 - Livewire Background

Wirewalkers are profiling vehicles that use the motion of surface waves to move vertically in the water column. Sensors housed within the Wirewalker record continuous data as it ascends freely to the surface buoy. Onboard sensors typically record high bandwidth data to gather detailed vertical and time-resolved information, which is possible over long time periods since profiling expends no energy. Nevertheless, deployment duration is limited by onboard battery energy used to power sensors (Pinkel et al. 2011). Plots below from a year-long study in La Jolla Canyon show the spatial resolution capabilities when examining individual internal waves passing the profiler (Fig. 1). The high-resolution data can show small scale wave dynamics over hours, and the yearlong study reveals how they change seasonally. In this study, the Wirewalkers were recovered and re-deployed every three weeks. Doing so required expensive ship-time and the synchronization of different datasets–a time consuming, and thus, costly task (Lucas et al. in prep).

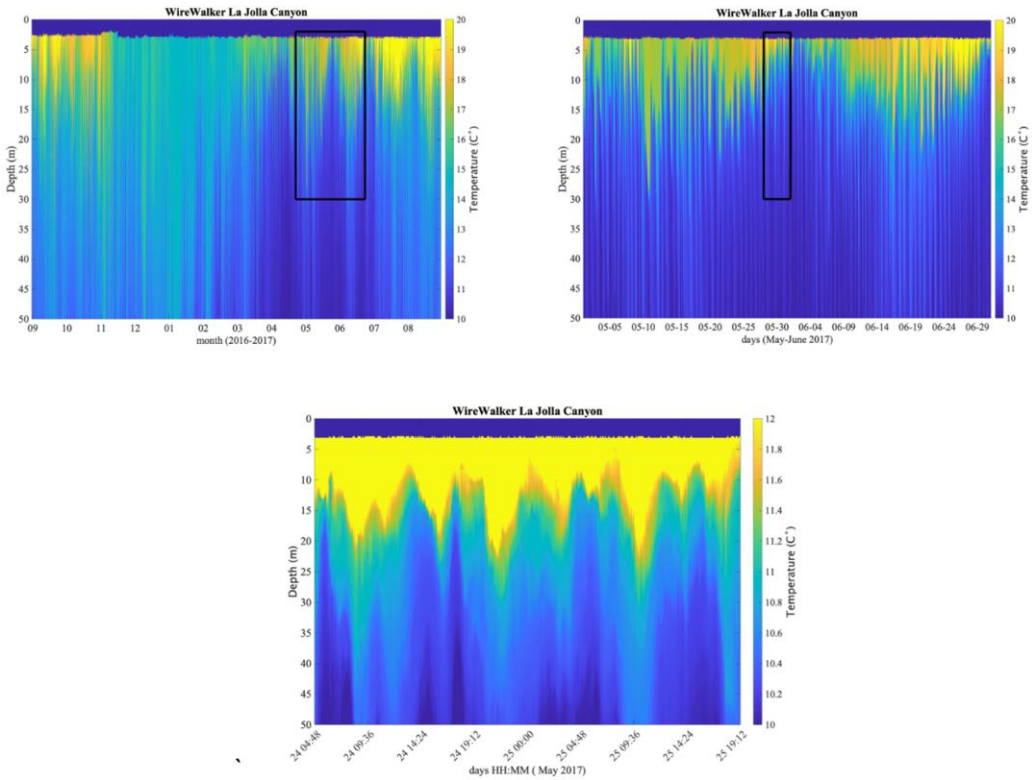

Figure 1: Temperature (°C) of the upper 50 meters of the water column in La Jolla Canyon for 1 year, 2 months, and 1 day. Courtesy of Drew Lucas and Arnaud Le Boyer `

The Wirewalker system has no electronic components, instead relying on the relative motion of the buoy and the profiler to move up and down the wire with a mechanical cam. A passing wave pulls the mooring wire upwards as the buoy floats to the crest, but, since the profiler has significant inertia, the cam allows the profiling wire to move relative to the profiler, having the effect of rectifying the orbital motion of ocean surface waves into uni-directional travel (Pinkel et al. 2011). The profiler climbs down the wire at 10-20 meters per minute until it reaches the bottom, disengages the cam, and floats the surface as shown (Fig. 2). The cam disengages by hitting a rubber bumper near the bottom of the mooring wire, and then floats up at about half a meter per second until it hits the bumper at the top to re-engage the cam. The free ascent of the Wirewalker allows the on-board sensors to record smooth and continuous data through the water column.

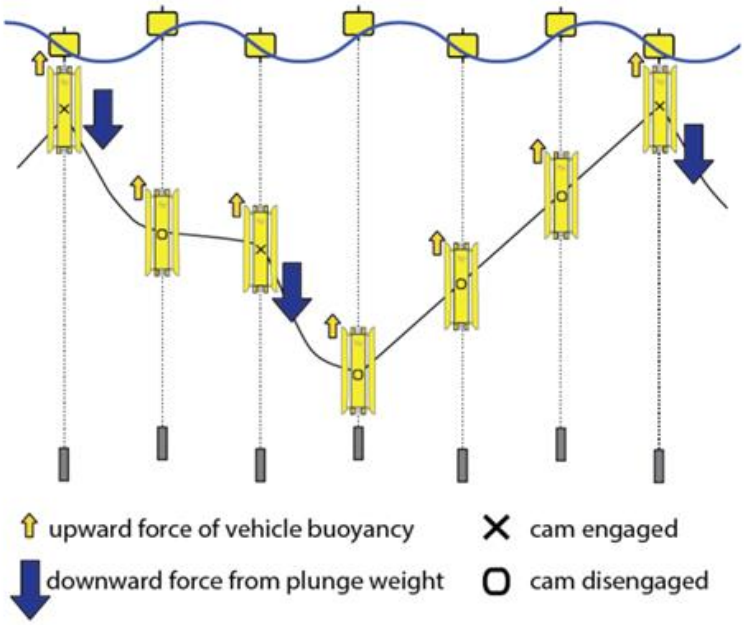

Figure 2: Wirewalker camming diagram courtesy of Del Mar Oceanographic, LLC ("The Wirewalker: How It Works" n.d.). The cam locks onto the wire for the downstroke of a wave. The mooring wire is held vertical by weights.

Researchers at Scripps Institution of Oceanography and elsewhere have shown that Wirewalkers are reliable after two decades of research and development. The Office of Naval Research (ONR) sponsored "Livewire" project aims to replace the large batteries with a wave-powered generator that can increase deployment times, profile in extremely calm conditions, and target specific depths to profile. MOD has developed a prototype motor/generator that can communicate rotational velocity via Hall effect sensors. Here, I present my efforts to merge the generator with existing Wirewalker technology to build a functioning Livewire prototype (Fig. 3). The generator and "Power Take-off" will replace the v-groove cam by controlling the load torque required to spin the generator instead of mechanically locking onto the wire—a fundamental redesign of the Wirewalker (Fig 4).

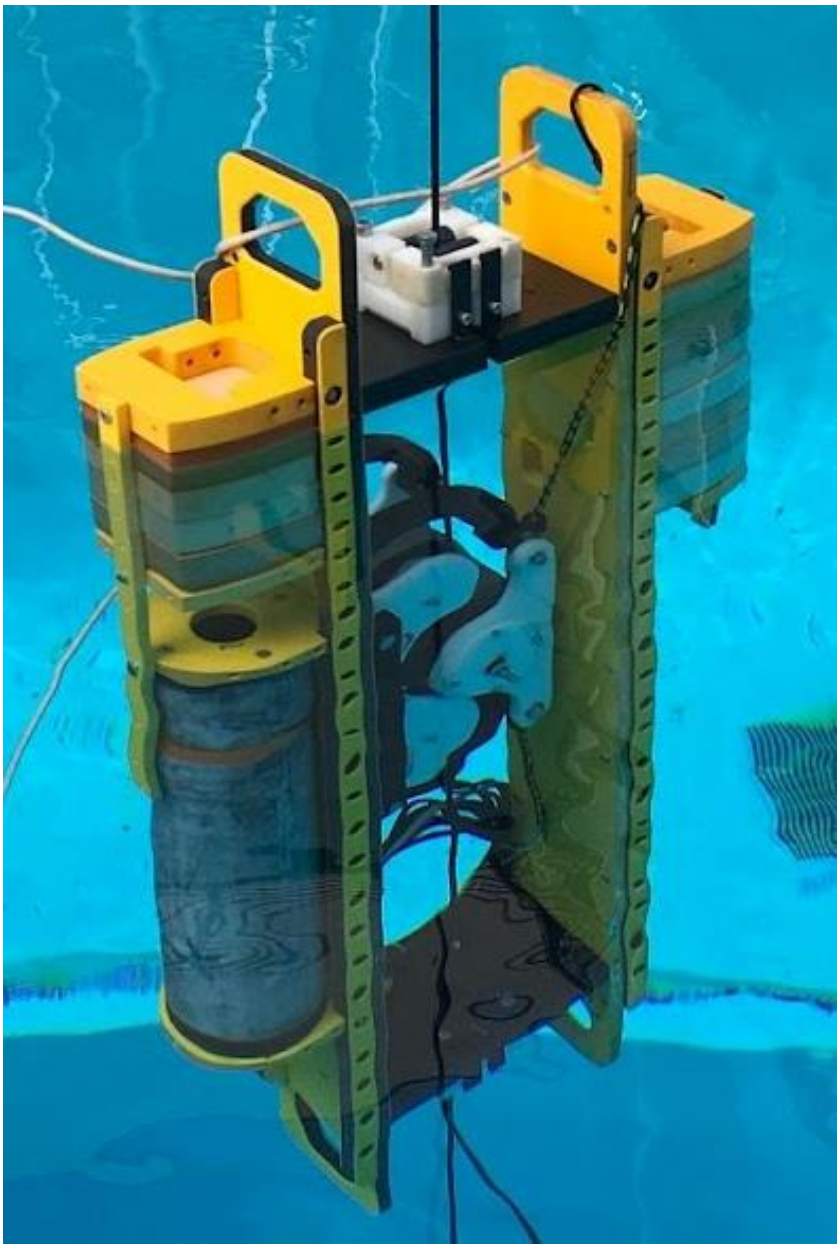

Figure 3: Photograph of Livewire prototype in the Keck test pool courtesy of Ewan Bohannon. The Power Take-off (center) is controlled by a circuit in the pressure case (left) from within the profiler frame.

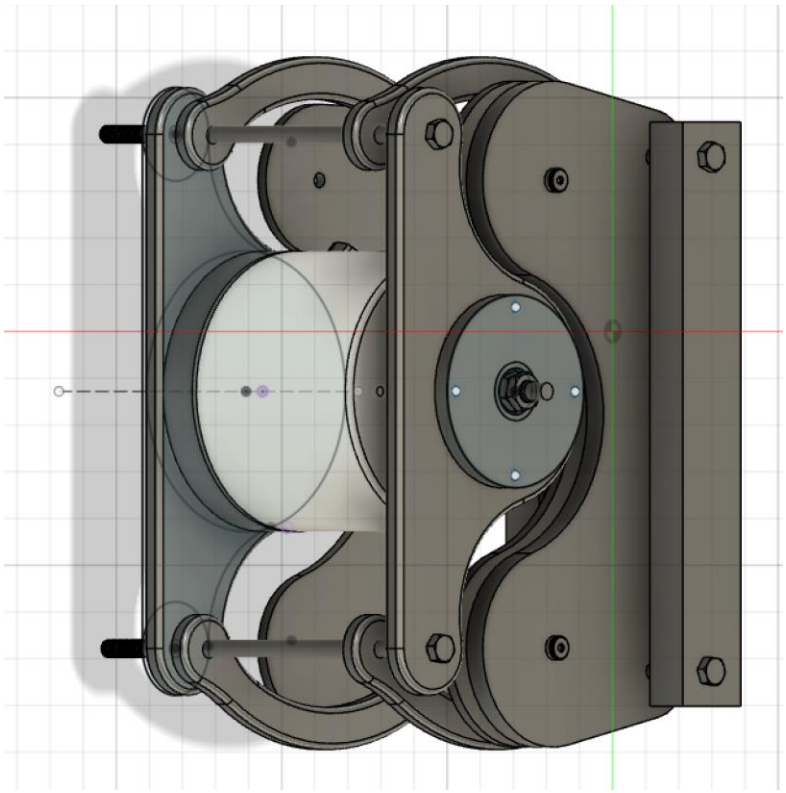

Figure 4: Rendering of the 3-wheeled Power Take-off by Thomas Kelly with submersible generator rendering courtesy of Jonathan Ladner.

1.2 - Livewire Dynamics

Wirewalker dynamics balance drag and buoyancy with a motion forced by the linear wave equation from Pinkel's 2011 "The Wirewalker: A Vertically Profiling Instrument Carrier Powered by Ocean Waves". The Wirewalker mechanical cam could be approximated as perfectly coupled to the wire or perfectly uncoupled, but the Livewire cannot. The Livewire generates power from the relative motion between surface waves and the profiler. In both coupled and uncoupled states, there will be a difference between the wire motion and the profiler motion. The Livewire does not lock like the mechanical cam, it slows the wire by increasing work required to spin the generator. While the simplified camming dynamics are like the Wirewalker which moves down by coupling at the peak of a wave and decoupling at the bottom, the Livewire may delay camming to take

advantage of the high accelerations at the peaks and troughs to generate power. Also, the Livewire cannot fully decouple from wave motion because the wire is always spinning the generator. Only by reducing the torque needed to spin the generator is the profiler able to achieve one-way travel. The dynamics are continuous since the generator is always spinning, until it starts to slip in the wire.

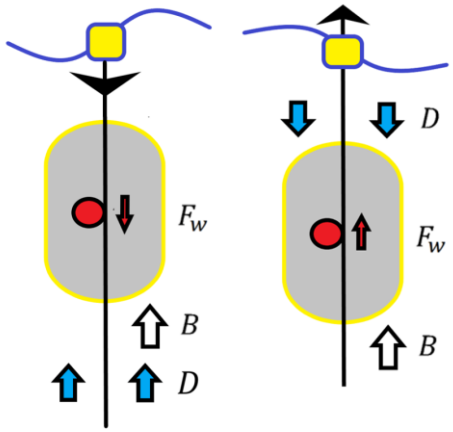

Figure 5: Livewire free body diagram illustrating drag (D), buoyancy (B), and the wire force (F_w) on the profiler.

The wire spins the generator but is resisted (F_w) by the generator's load and rolling resistance (Fig 5). The load torque is controlled by varying the load resistor (R) in the circuit connected to the generator (Eqn. 1).

$$T_{load} = k_g^2 R\, \varpi_{gen} - \mathrm{k_g V_{in}} \qquad (1)$$

The generator can act as either a motor or a generator. When the voltage into the windings ($\mathrm{V_{in}}$) (Eqn. 1) is zero and the rotor is turned (ϖ_{gen}), the motor-generator will be generating power. The constant ($\mathrm{k_g}$) is a fixed property of the motor-generator (Austin 2019).

The rolling resistance is associated with the energy dissipated from the deformation of the 95a polyurethane wheel. The rolling resistance coefficient of friction is proportional to the rolling velocity (v) relaxation time of the material (τ), and inversely proportional to the radius of

curvature (R) (Popov 2017). Eqn. 2 below describes a deformable cylinder on a flat rigid body, but it is used to approximate the deformable cylinder on a perpendicular cylindrical rigid body (Popov 2017).

$$F_{R,fr} = N * \frac{3}{4} * \frac{v\tau}{R} = N * \mu_{rolling} \quad (2)$$

Table 1: Livewire dynamics variable definitions

Variable	Symbol	SI Units
Generator wheel radius	R	m
Generator constant	k_g	V-s
Rot. velocity of gen.	ϖ_g	Rad/s
Rot. acceleration of gen.	α_g	Rad/s^2
Moment of inertia of rotor	I_g	Kg-m^2
Motor/gen. input voltage	V_{in}	V
Sliding velocity	v	m/s
Relaxation time	τ	s^{-1}
Load torque	T_{load}	Nm
Rolling friction	$F_{R,fr}$	N
Profiler-wire force	F_w	N
Normal force on wheel	N	N
Coefficient of rolling friction	$\mu_{rolling}$	-
Coefficient of sliding friction	$\mu_{sliding}$	-
Wave frequency	σ	s^{-1}
Wave Amplitude	A	m
Vertical wave velocity	w_{wave}	m/s
Relative velocity of the wire to the profiler	w_w	m/s

Here it is assumed that the wire's force on the profiler is from the contact on the generator wheel, neglecting friction from the sheaves and roller guides. The vertical force of the wire on the profiler loads the generator to induce rotation by overcoming rolling friction and the rotational inertia

$$\Sigma \mathrm{M}_{\mathrm{Wheel}} = F_w R - N * \mu_{rolling} R - T_{load} = \alpha_w * I_{gen}$$
$$F_w = \frac{T_{load}}{R} + \alpha_g * \frac{I_g}{R} + N * \mu_{rolling} \quad (3)$$

When the vertical force from the wire onto the profiler exceeds the sliding friction, the profiler wheel will slip instead of roll. This creates an upper bound for F_w. The above force balance is neglecting other sources of friction on the profiler, which could be added here if found to be significant.

$$F_w = \begin{cases} \frac{T_{load}}{R} + \alpha_g * \frac{I_g}{R} + N * \mu_{rolling}, & (0 < F_w < N\mu_{sliding}) \\ N * \mu_{sliding}, & (F_w > N\mu_{sliding}) \end{cases} \quad (4)$$

In the no-slip regime, the rotation of the generator follows the mooring wire driven by vertical velocity of waves at the surface as described by linear wave theory (Kundu 2015).

$$w_{wave}(t) = \sigma \mathrm{A}\cos(\sigma t) \qquad \text{at z=0} \quad (5)$$

The vertical velocity of the wave moves the profiler, but the effect decreases with depth because the pressure perturbations from the surface waves decrease exponentially at depths past the wavelength. In deep water waves, the ratio of depth to wavelength is high ($\frac{h}{\lambda} \sim kh >> 1$), so the circular wave orbital radius decreases with depth from the surface (-z) (Eqn 6). In shallow water waves, the ratio (kh) is low, which causes the vertical component of the orbital to decrease with depth (Eqn 6), but not the horizontal component (not seen) (Kundu 2015).

$$w_{wave}(t) = \sigma \mathrm{A} * \frac{\sinh(\mathrm{k(h+z)})}{\sinh(\mathrm{kh})}\cos(\sigma t) \quad (6)$$

The profiler is driven by the relative motion between the surface wave and wave orbitals at the profiler's depth (Pinkel et al. 2011).

$$w_w(t) = \sigma A \cos(\sigma t)\left(1 - e^{-k(\sigma)z}\right) \quad (7)$$

For one-way motion, the generator torque term (T_{load}) needs to have a large effect on the acceleration of the profiler. To stay still in the water column, the profiler's inertia and form drag needs to overcome the generator inertia and rolling friction. To move, the combined forces from the wire need to overcome drag. For this aspect, and the frictional gripping force (or more formally the sliding friction) is great enough to prevent slipping from waves.

CHAPTER 2: Design and Fabrication 3-wheel Power Take-Off

The Livewire cable drive system is a 3-wheel Power Take-off designed to maintain traction and minimize rolling friction (Fig. 4). Frictional losses reduce the energy generating potential and impair vertical profiling. 2-wheeled pinch roller and 3-wheeled hinging designs were built and tested to find the coefficient of friction and explore methods to decrease rolling friction without slipping. The 3-wheeled power take-off has only one 95a polyurethane wheel and two sheaves that distribute pressure around the wheel in an "omega configuration" with force that is a fraction of the wire tension. To make the power take-off more robust, a hinging action and beam springs were introduced to increase the normal force on the wire in heavy wave (and peak demand) conditions and allow the frame to deform before breaking. Based on results from generator power tests, land-based hanging experiments, and FEA studies, the power take-off was strengthened and better constrained in preparation for a final proof-of-concept pool test.

2.1 – Coefficient of Friction Test

The hertzian contact mechanics and FEA of the Livewire wheel and wire was described in 2019 (MOD, 2021). FEA simulations concluded that 143 lbf of normal force would produce the best grip on the wire because the wheel would deform all the way around the wire to maximize contact area. The vertical gripping force was estimated to be 43 lbf from calculating $F = \mu N$ with an assumed coefficient of 0.29. A central conclusion of this early analysis was that it needed to 1) be confirmed by laboratory test and 2) that this laboratory test be repeated in wetted conditions, since the 95a polyurethane and the plastic coating on the tensioned wire would both likely have different coefficients of friction in dry vs. submerged conditions.

The COF experiment compared the wet and dry wire gripping force of the 95a polyurethane wheels envisioned for the Livewire. A hanging dynamometer measured the force required to pull

the wire through a test jig with locked wheels (Fig. 6) The wheels were pinched tighter to vary the normal force, but force was not directly measured. Instead, the normal force was calculated from deformation of the 95a polyurethane. Deformation was measured as the distance between the outside axles of the wheels, minus the diameter of the wheel, wire, and axle bolt. COF decreased from 0.27 to 0.17 when the test jig was submerged in seawater.

Measuring the maximum gripping force was challenging because the wire slipped very slowly even at low loads, then the maximum force would jump over 100% if the wire was pulled through quickly. Measurements were averaged and the wire was pulled as slowly and consistently as possible to reduce the variability.

Methods

The test jig consisted of aluminum angle extrusions on either side of both wheels, that share an axle on the bottom and have 1" aluminum stock on the other. The aluminum stock has a slot for the wire, and a ¼-20 tapped hole for a screw to tighten the vice together (Fig. 6). The second piece of aluminum stock has a through hole for the screw. Bushings were made to press-fit the wheels onto an axle, and pins were put in holes drilled into the wheels to prevent them from rotating.

Figure 6: Pinch-roller model and coefficient of friction test setup without water. Dynamometer forces were recorded as the hoise pulled the wire section out of the jig.

The test jig was tied to an anchor in a plastic drum and held upright by a short length of coated wire attached to the hoist (Fig. 6). A dynamometer was zeroed with the wire, but without the jig. Each test began with the jig held upright by the wire. The wire was taped to make slipping clear. A caliper measured the distance between the axles of the wheels, which stepped tighter by increments of 0.05”. The deformation of the two wheels was calculated as the sum of the wheel, wire, and axle screw diameters minus the distance between outside of the axles when tightened together.

A hand-driven hoist slowly pulled wire out of the jig. The maximum force was recorded before the wire started to slip, and a second dynamometer reading was recorded as the settled tension when the wire stopped slipping. The experiment continued by resetting the wire, changing the wheel's displacement by tightening the screw, and repeating the pull test. First, a dry friction test helped narrow the scope for the wet test to the distances most likely used in the Livewire design. In the wet test, five set displacements were averaged three times each for consistent data.

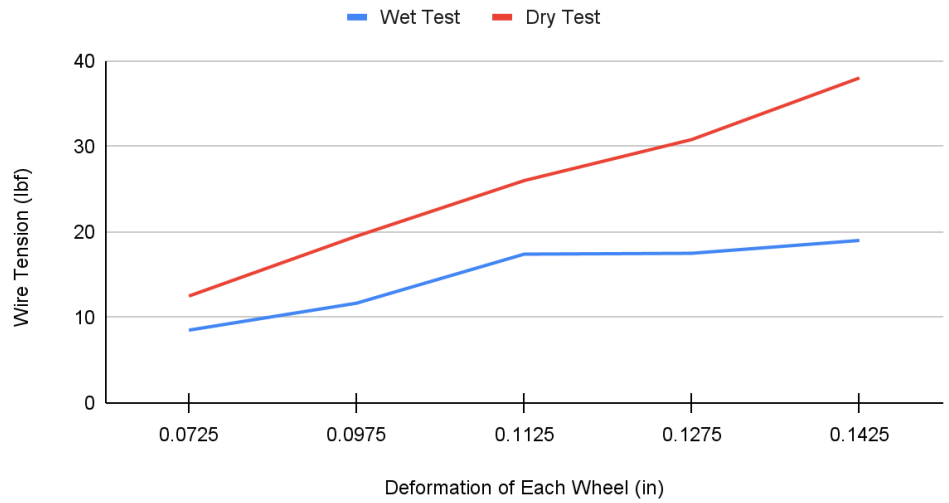

Figure 7: Vertical Wire Grip (lbf) vs Deformation of Each Wheel (in) measured with the maximum tension from a dynamometer and from the change in axle-to-axle distance in dry and submerged tests.

The maximum wet tension was on average 58% that of the dry, and it increased at half the rate of the dry test as wheels were moved tighter together (Fig 7). The change in tension over change in deformity is related to the coefficient of friction through the elastic properties of the wheels. It was assumed that the experiment remained in the elastic domain of the 95a polyurethane, but that was challenged by small grooves worn into the wheels at high tensions. To address this, the wheels were rotated for a new test surface whenever inelastic deformation was noticed.

Discussion

The coefficients of friction were found using the theoretical normal force needed to elastically deform the wheels and the gripping force from the dynamometer (Eqn. 6) (Popov 2017). Normal force is related to the elastic deformation of the urethane by the effective Youngs modulus (E^*) and effective radius ($\tilde{R}$). The dry test found the coefficient of friction to be 0.27 by averaging the 5 gripping forces from wheel deformations between 0.0825” and 0.1425”. This corresponded to dry gripping forces between 14.5 and 38 lbs. The same test was submerged in saltwater and found an average wet coefficient of friction to be .17. The gripping forces when wet were between

8.5 and 19 lbs. These metrics are from the maximum tension during slow pulls. The settled tensions with slightly lower coefficients—wet COF was .11 and dry COF was .17.

$$\text{Normal Force: } N = \frac{4}{3} E^* \tilde{R}^{\frac{1}{2}} d^{\frac{3}{2}} \tag{6}$$

The coefficient of friction increased as the wheels deformed for the dry test, but not the wet test. The additional contact area from deforming around the wire helped prevent slipping in the dry test, suggesting that a soft, deformable wheel is advantageous. The wet test saw increasing coefficient of frictions up until the deformations around .1275," then the coefficient decreased (Fig 8) (Fig 9). The decrease in wet COF is likely from inelastic deformation at high normal forces creating a groove in the wheel (A 1).

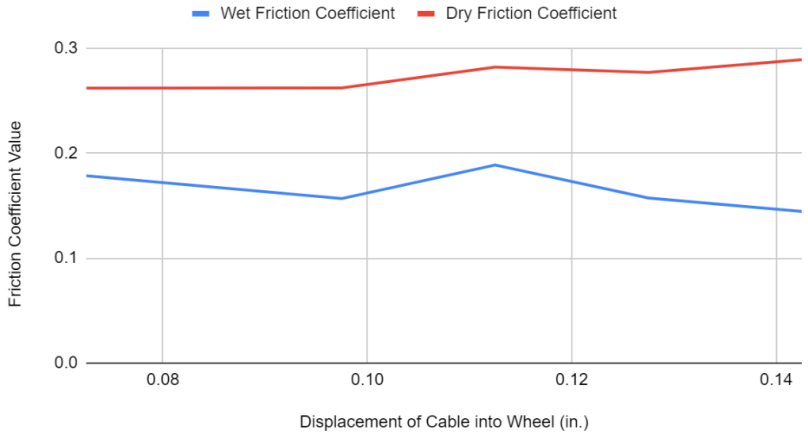

Figure 8: Coefficient of Friction vs Displacement of the Wire (in) into Each Wheel for maximum tension measurements. The coefficient of friction is constant as the deforming wheel wraps around the wire.

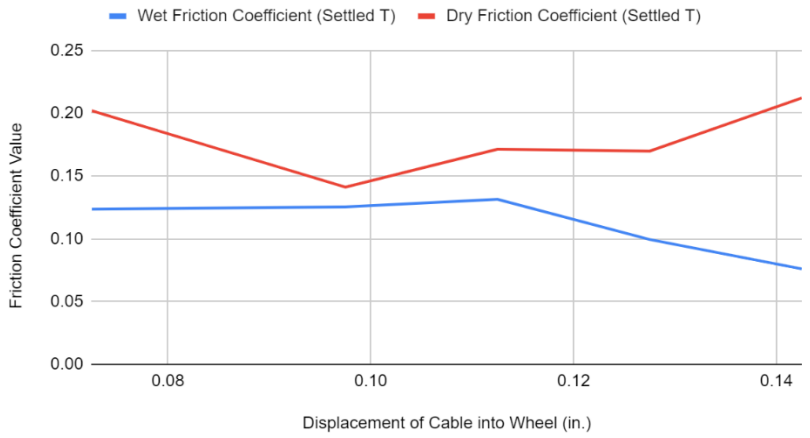

Figure 9: Coefficient of Friction vs Displacement of the Wire (in) into Each Wheel for settled tension measurements. Variability of the coefficient of friction is likely due to experimental error.

Uncertainty was introduced from the lack of uniformity between test pulls. The wheel's grip on the wire was much higher for impulsive loading than constant loading. When pulled quickly, the maximum tensile force on the wire reached double the slow pull. After several tests, the wire wore a groove in the 95a polyurethane wheels which let the wire slip through at low speeds (A 1). To account for this, we rotated the wheels and drilled a new hole to lock them.

Adding more wheels to the design would reduce wear by increasing the frictional contact area on the 95a polyurethane. Stiffer, stronger wheels could reduce slippage and frictional losses in the system due to inelastic deformation. Also, the Hertzian contact model suggests that a larger wheel would increase the effective radius of the cable-wheel pair and increase the normal force for a given displacement (Popov, Heb, and Willert 2019).

2-wheel Drop Test

Drop tests confirmed that the deformation of the wheels created rolling friction that resisted motion even when the wheels were free to rotate. The low COF requires higher normal forces to grip on the wire, which increases losses due to inelastic deformation. Rolling friction is an energy loss due to elastic hysteresis when the energy of deformation is less than the energy of recovery.

The test wire was attached to 12.5 lbs of weight and recorded as it pulled through the free-spinning jig. First, the jig was prevented from spinning with a pin and tightened until it could barely hold up the weighted wire. Then displacement was measured from axle to axle as done in the friction tests. Each wheel deformed by .085" inducing a normal force of 47.7 lbf (Eqn. 6), which requires a dry C.O.F. of 0.26 to hold up the 12.5 lbs. When the pin was removed, the weight fell 45 cm over 0.55 seconds with an acceleration 3.03 m/s^2. Assuming no-slip conditions, the balance between gravity, rolling friction, and the rotational inertia of the wheels leads to a rolling friction of 38 N compared to the static friction of 55 N to hold the weight with the pin. The bearings continued to spin long after the wire fell through, inferring that most of the losses were from hysteresis in the 95a polyurethane.

The test jig was in the same position when holding the weight with static friction and after the pin was pulled, so the normal force for rolling friction and static (or sliding) friction is assumed the same. With the same normal force, the ratio of rolling friction to static friction is the ratio of the coefficients. From this test, the coefficient of rolling friction is 69% the coefficient of sliding friction for the 95a polyurethane wheel. A maximum of 31% of the force from wire into the Power Take-off would be loading torque into the generator (Eqn. 4). Also, the rolling friction would act as a constant coupling force on the wire, preventing 1-way travel. Even though the early design process was exploratory, future experiments should be more formalized to validate design

decisions. Despite the uncertainty, the drop tests showed the necessity of new cable drive systems that do not rely on a pinch roller or static normal force.

2.2 – Variable Force Power Take-off

The variable force Power Take-off, or "omega drive" proposed with the help of Michael Goldin, has 3 wheels, and aims to mechanically increase the normal force as the wire accelerates, to address the aforementioned rolling friction implicit in a pinched wheel design. The "omega configuration" offsets the tensioned mooring wire to create the horizontal normal force on the generator wheel. This is combined with a hinging action to allow the generator to swing in between two idler sheaves. As the generator is pulled up or down by the wire, its grip tightens on the wire. The generator wheel has an arced path that moves inward as it hinges, pushing harder against the wire section between the sheaves. This hinging action synergizes with the generator torque control. When the profiler needs to stay coupled to the wire, the generator torque increases, causing it to swing up or down with additional force to better grip the wire. This action is a positive feedback loop that passively clutch helps the Livewire grip the wire when necessary, without increasing the constant normal force and associated losses.

A 3-wheel "omega-drive" Power Take-off has a better grip and less rolling friction than a pinch roller because it distributes the forces and makes use of the Capstan equation. The pressure from the mooring wire is distributed around a larger contact area on the 95a polyurethane wheel determined by the offset angle (omega)(Popov 2017). The 95a polyurethane idler from the pinch roller is replaced by two HPDE sheaves that should help reduce energy losses because the sheaves are not meant to deform or grip the wire. Whereas the contact mechanics of a pinch roller could be approximated by two cylinders on a flat rigid body (Eqn 7), the coefficient of friction will change to account for the geometry of contact on the generator wheel and friction from the sheaves.

The rolling friction equation (Eqn. #?) is assumed to remain a function of the normal force from the horizontal components of tension.

The Power Take-off is dependent on wire tension. The normal force on the generator wheel is the horizontal component of the wire tension when offset by the sheaves (Fig. 10). For small angles, the frictional contact between the wire and the wheel can be approximated by the horizontal component of wire tension and COF.

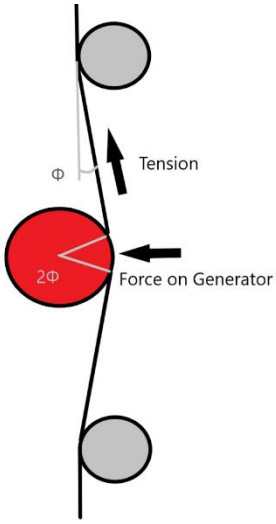

Figure 10: Omega configuration free body diagram of the generator wheel and sheaves. The normal force responsible for the frictional contact on the wire is a fraction of the tension depending on the offset angle.

The normal force approximation becomes less accurate as the wire bends further around the sheaves. The Capstan equation (Eqn. 8) accounts for the exponential increase in holding force (F_{hold}) compared to the load (F_{load}) when a line wraps around a cylinder (Popov 2017) from the offset angle (φ). Figure 11 shows the similarity of a normal frictional force and a cylindrical frictional force at small angles, and the divergence at larger angles. The non-dimensionalized force term is the frictional gripping force from the clutch ($F_{s,fr}$) as a fraction of the wire tension from the corrected mass of the bottom weight in seawater ($m_w^* * g$). It should be noted that this model does not account for other forms of friction from the sheaves, bearings, or roller guides. In practice, these would add up to increase the profiler resistance to rolling on the wire.

$$F_{load} = F_{hold} e^{\mu_s 2\varphi}$$
$$m_w^* g + F_{s.fr} = m_w^* g e^{\mu\_s 2\varphi} \tag{7}$$
$$\frac{F_{fr}}{m_w^* g} = F_{fr}^* = e^{\mu_s 2\varphi} - 1$$

$$F_{s,fr} = N\mu_s$$
$$F_{s,fr} = 2 * \sin(\varphi)\, m_w^* g * \mu_s \tag{8}$$
$$\frac{F_{s,fr}}{m_w^* g} = 2 * \sin(\varphi)\mu_s$$

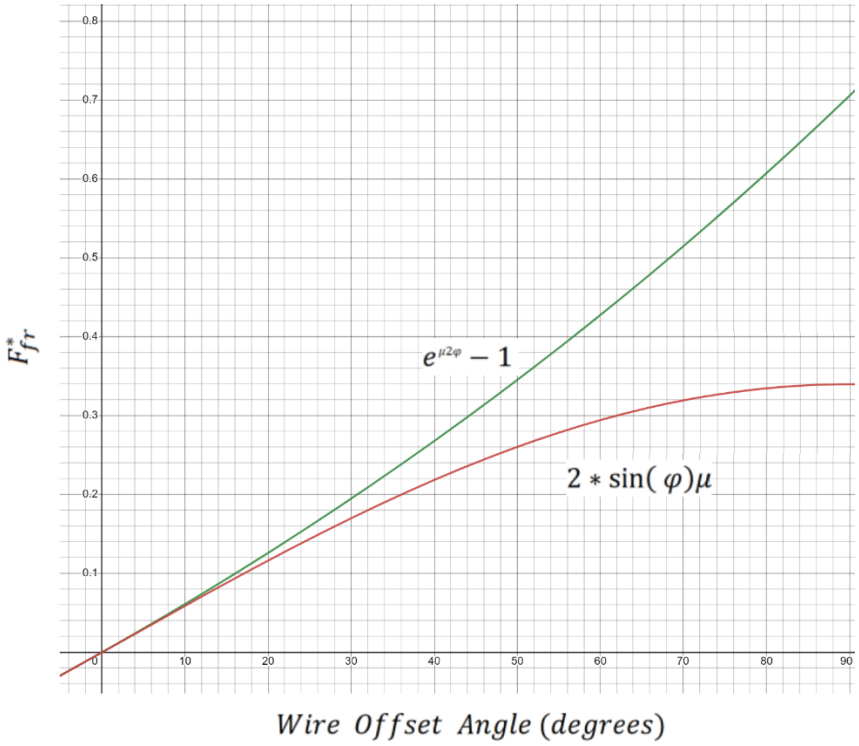

Figure 11: Frictional gripping force as a fraction of the wire tension versus wire offset angle relative to vertical with a COF .17 for a cylindrical surface (green) and a normal surface (red)

Design Process

The Power Take-off was constrained by size and practicality to work in a retrofitted Wirewalker frame. The Wirewalker frame was only widened as needed to fit the generator and sheaves to reduce drag from profiling and currents. By minimizing the length of the connecting

acetal bones, the hinging action was diminished. Acetal was chosen for load bearing plastic pieces for its strength to minimize the size and weight.

The profiler had to easily attach from the mooring wire for a user-friendly experience in the field. This was accomplished by putting the bones in line with the generator, behind the 95a polyurethane wheel (Fig. 12). The wire could be placed into the Power Take-off without removing any pieces. The Delrin acetal faceplates were made larger than the sheaves to reduce the risk of the wire popping out. When the wire was centered on the Livewire frame, the generator stuck out to the side. This imbalanced the system but high tensioned mooring wire kept it upright. The HDPE spine bars attach to the structural wall of a retrofitted Wirewalker frame which keep the sheave plates fixed while allowing the swinging of the generator.

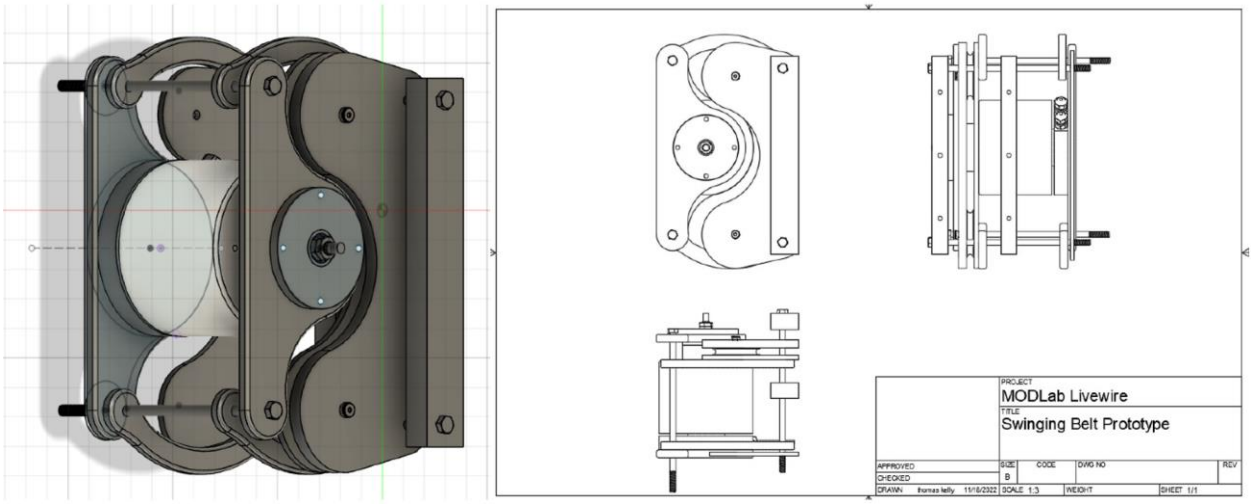

Figure 12: 3-Wheel Power Take-off model and drawing by Thomas Kelly.

The Power Take-off pushes the wire 11° off from the vertical. This wraps the wire around the 22° of the generator wheel and pushes on it with 38% of the wire tension, assuming no deflection (Fig. 12). It provides about a 1:10 holding force to wire tension in dry air with a COF of 0.27. When wet, the holding force is only 6.5% of the wire tension due to the .17 COF from the

static friction test. The low holding force should have been addressed in the design phase, but proof-of-concept from the dry test encouraged progress towards testing in the water.

Manufacturing Process

The manufacturing process was a multi-step challenge to reduce friction and fully constrain the Power Take-off (Fig. 13). The acetal generator plate fits over the wheel and was screwed onto a circular puck containing a shaft bearing. The combination of plate and puck kept the mooring wire from slipping off the wheel. Stock HDPE Sheaves were machined by lathe to house two low-friction ceramic bearings, and tightly constrained between acetal plates to fit around the generator. The 8mm bearings were compressed by a shoulder bolt through the acetal plates with plastic spacers on the outside and between the bearings. The acetal plates centered the sheaves on the generator wheel, requiring the back plate to be very thin. Pockets for the sheaves were machined into the plates to reduce the width and help prevent the wire from slipping out of the u-shaped sheave track. The viscous shear effects of water between the spinning sheave and the plate were estimated using Couette flow from a vertical speed of 0.5 m/s and gap of 0.05”. The forces due to shear were 0.009 N for each side of a sheave and subsequently ignored.

Each moving piece of the hinge had a brass bushing and was separated by washers and acetal spacers to compress and constrain the 10” by ⅜” 316 stainless steel connecting bolt. The bushings and washers kept the hinging movement free when the spacers on the bolts were compressed. Since the clutch was free to hang, elastic lines on the top and bottom hold the generator in a neutral position in air.

Figure 13: Power Take-off prototype on the widened Wirewalker frame.

The Livewire generator center shaft rotates in a 16mm ceramic bearing in the circular acetal puck pictured above. The Power Take-off frame compresses the generator shaft inward to constrain the internal angular contact bearing between the rotor and stator. The external surface and wheel surround the rotor, while the center stator connects only to the back. The back of the stator could be bolted directly to an acetal plate to fully constrain the generator. To accommodate the generator and omega drive system, the Wirewalker frame had to be widened from 4” to 10.5” between the structural walls.

If the 3-wheel Power Take-off design was remade, the sheaves should be a stronger material and the acetal plate better constrained. This was the weakest point of the design because

the thin plates and HDPE sheaves rub together when loaded too tightly or slightly misaligned. In the final pool test, a sheave's bearing pocket was warped to the point of seizing by misaligned loading. Once the 3-wheel Power Take-off was built, the electronic side of the project became center focus to test the Livewire.

2.3 – Power Curve Test

The Livewire power curve test empirically found the ideal load resistance by driving the generator with an external motor and plotting the power against rotational speed and load resistances. The Maximum power transfer theorem states that the most efficient load resistance is equal to the source resistance (Harrison 2013). The load resistance controls the load torque, and thus how tight the Livewire must grip the wire to prevent slipping through the wheels. In this experiment, the Livewire generated the most amount of power with a 4-4.5 Ohm load from 70 to 120 RPM. Future tests will evaluate if the 3-wheel design can cam along the wire by switching between 4-4.5 Ohms and an open circuit to vary the load torque.

Methods

The Livewire generator was driven by a motor and wired to a rectifier then a resistor (Fig.14). The voltage was measured across the load resistor with a multimeter to calculate power. In the final experiment, lower resistance wires and connectors replaced smaller wire and clips to ensure that the voltage measurements were across nearly 100% of the system load. Any extra resistance from the circuit would make the source resistance seem larger, which biases the result higher for ideal load resistance. The photo of the test setup below shows the motor, generator, multimeter, and resistor on the table, while the blue bin contained wire connections and an AC to DC rectifier.

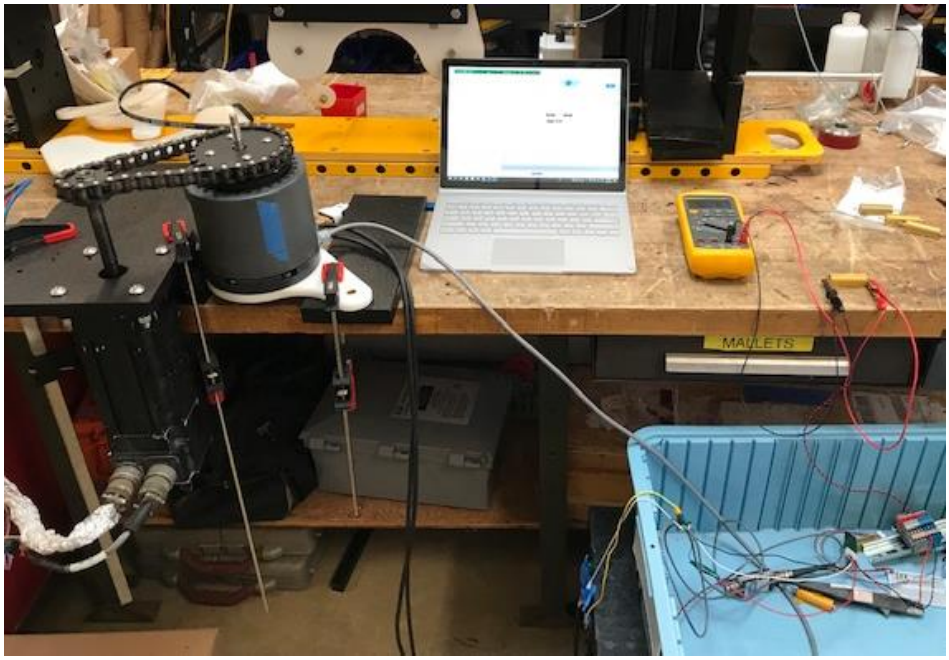

Figure 14: Power Curve test bench setup with the driving motor, generator, Elmo Harmonica on the laptop, multimeter, and load resistor (left to right).

An Elmo Harmonica drove the motor at varying RPMs as commanded through the Elmo Composer software to show that maximum power from the generator occurs at the same load resistance at every speed. In the first attempt of the experiment, a timing belt and pulleys were fixed on the shafts with set screws. The set screws failed to prevent the pulleys from rotating and scratching the shaft. Chain and sprockets replaced the timing belt to accommodate for larger inner diameters from screw-clamp bushings, and the convenience of off-the-shelf parts. The chain and sprocket may have been excessive, and future experiments could be done with a timing belt. The Livewire generator shaft started to slip by rotating in its press fit, so the screw clamp bushing was removed, and a mount was created to connect the sprocket to the generator body.

Results

The first set of tests succeeded in narrowing down the range of loads and motor speeds but suffered from low quality circuit connections which added resistance and biased the results. The

added resistance from the circuit artificially increased the source load, making the ideal resistance seem too high. On the graphs, the rotational speed of the generator was converted to vertical speed of the Livewire (Fig. 15).

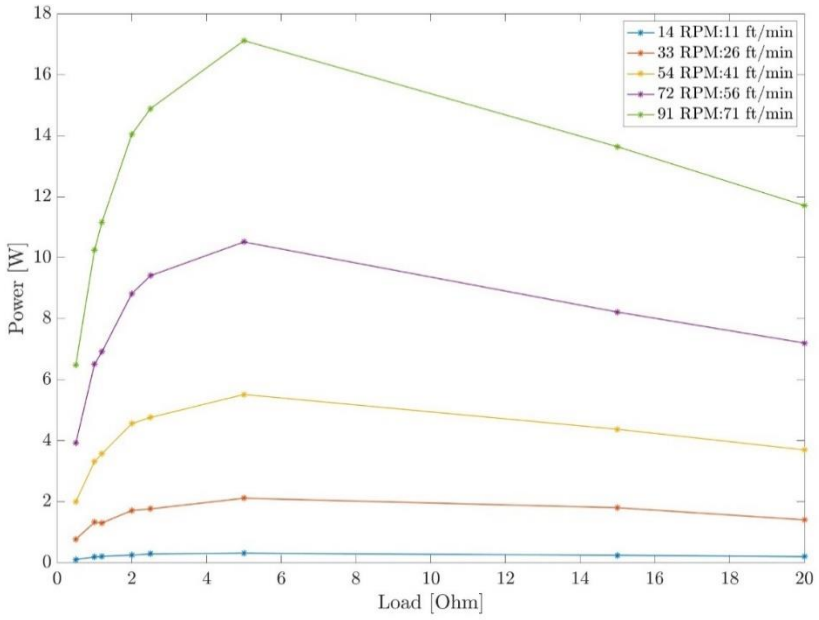

Figure 15: Generated Power (W) vs Load Resistance for five generator rotational speeds and the corresponding profiling speed assuming no-slip rolling. Power curve is biased by high-resistance wiring and contact, overestimating the ideal load resistance.

The second test achieved higher resolution with 7 points over 3 ohms and more accurate results from better wiring (Fig. 16). The second graph zoomed in over the peak resistances from the first test. The resulting power curves show that the most power is transferred to the load when it has a resistance between 4 and 4.5, regardless of the speed of the generator. The ideal load resistance is an important metric to find early on because it defines the “loaded state” when the Livewire is generating the maximum energy for any given movement on the wire. The Livewire is tested around this “loaded state” because it is an inherent property of the motor/generator regardless of the Power Take-off design.

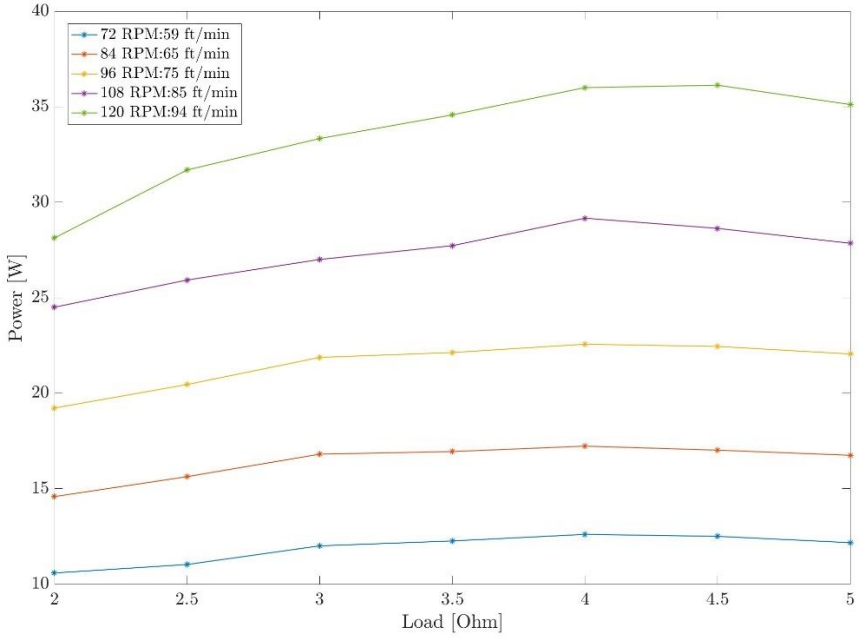

Figure 16: Generated Power (W) vs Load Resistance for five generator rotational speeds and the corresponding profiling speeds. Circuitry was improved and the test range was narrowed over the peak power output based on Fig. 15.

.

2.4– Dynamic Dry Test

The Dynamic Dry test was the first full scale experiment where the Livewire generated electricity from simulated wave motion on land. The force between the profiler and wire, F_w, was measured while changing the bottom weights from 10 kilograms to 70 kilograms. At each tension, the vertical force from the profiler was measured with an unloaded and a loaded electrical system. The loaded system had the most efficient generator torque by running the three phases from the generator through a rectifier and over resistors in series equivalent to 4.5 ohms. The unloaded system was an open circuit with zero generator torque.

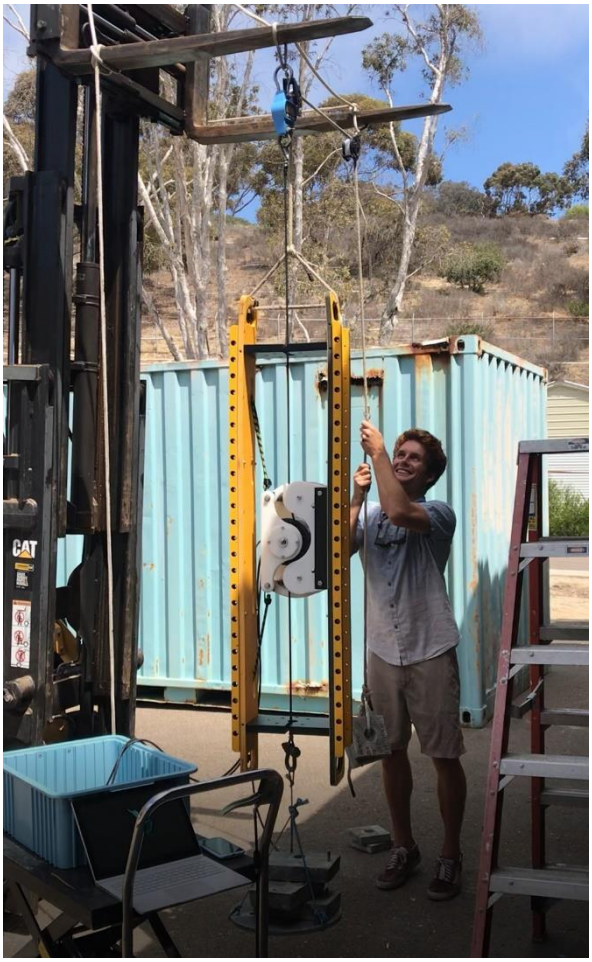

Figure 17: Photograph of dry test set-up courtesy of Tobi. The Livewire was moved with a counter-weighted offset rope, while the change in wire tension was measured with a dynamometer.

Methods

The assembled Livewire prototype was suspended using a counterweight on a tensioned ¼" mooring line. The system was suspended from a forklift, with two pulleys separating the counterweight from the Livewire (Fig.17). The test roughly simulated a wave by pulling up and down on the counterweighted Livewire. The generator wires ran to a bench setup, where a multimeter measured the voltage over the load resistor. The tensioned mooring wire had a dynamometer connecting it to the forklift, which measured the change in tension due to the profiler's force on the wire. Each data point was collected by incrementing the lead bottom weights

and recording the peak tension from a few wave cycles. The difference between the measured wire tension and the base wire tension is the Power Take-off's vertical force on the wire (Fig. 18).

Resistance to Rolling

The force on the wire (F_w) is high when the system is connected to the load resistor, and minimal when the circuit is open. When the circuit is loaded, the increased F_w is used to couple the profiler to the wire and pull itself up or down in the water column. When the circuit is unloaded, the profiler lets the wire pull through without much resistance so it may stay still. The difference between the loaded and unloaded circuits wire force is Livewire's capability to cam using wave motion.

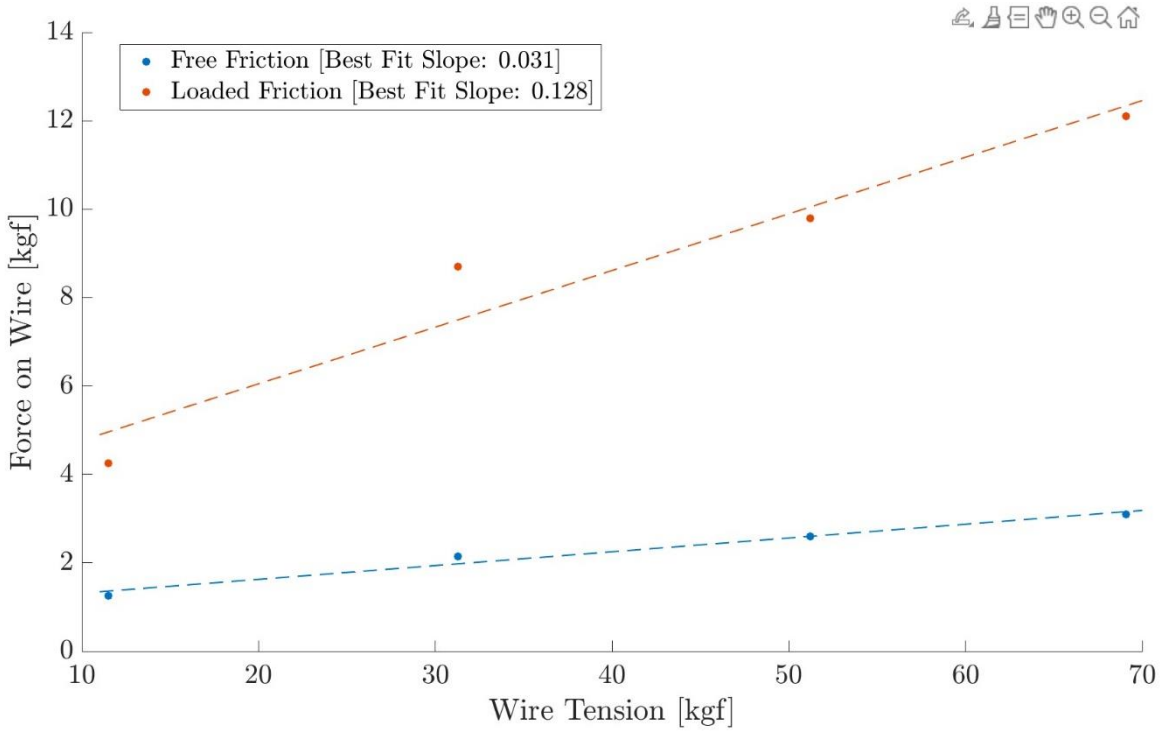

Figure 18: Livewire's Vertical Force (kgf) on the Mooring Wire depending on Wire Tension (kgf). As the profiler was lowered, the increase from base tension is the force on the mooring wire from the Power Take-off.

Wire tension has four times a greater impact on the loaded system than the unloaded system, which encourages higher wire tension for camming at the expense of power losses from friction (Fig. 18). The higher generator torque caused the force on the wire to surpass the upper

sliding friction limit, but the friction limit increased with higher wire tensions. The unloaded circuit unlikely surpassed the sliding friction limit, so small increase in F_w is from friction losses from the sheaves, bearings, and rolling friction over the generator wheel.

3-wheel Drop Test

The profiler was dropped about one foot, and the power over the load resistor was averaged for 3 runs with each bottom weight. A stopwatch timed the descent over a section of the wire. Greater bottom weights slowed the descent rate and decreased power generation because the normal force from the tension increased friction from the wheel and sheaves. Lower power output is a sign that the design is working as intended but losing efficiency. The loaded generator resists motion for the profiler to be pulled in one direction by the wave, while the unloaded generator allows rolling on the wire to stay still in the water column. Figure 18 is evidence that higher wire tension improves 1-way travel by increasing the difference between F_w of the loaded and unloaded Power Take-off. However, improving camming motion comes at a cost. Figure 19 from the drop test shows that the system loses efficient power generation with increased wire tension due to friction.

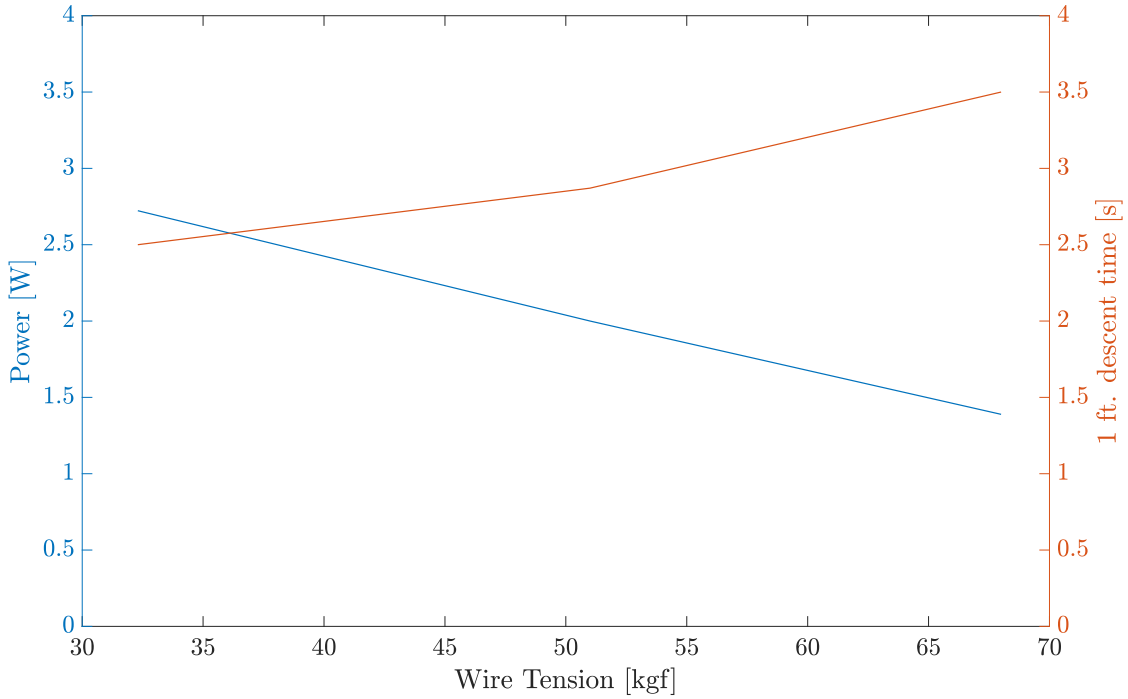

Figure 19: Generated Power (W) and Descent Time (s) versus Wire Tension (kgf) from Dropping the Livewire 1 foot in the Dry Test Setup.

The final Power Take-off will use a variable load resistance to effectively travel on the wire and generate power without losing efficiency. Instead of traveling deeper with a constant load torque during the downstroke of a wave, the Power Take-Off will increase load torque in phase with the velocity. The torque associated with a load resistance of 4-4.5 ohms is most efficient for generating power and will occur at the peak or trough of a wave making use of the surface wave's high accelerations. This load torque will not prevent rolling on the wire, but it will resist rolling to efficiently generate power from the relative motion from the wave and profiler. After the surface wave's peak acceleration, the load torque will increase to prevent rolling at peak velocities in the desired direction of travel by lowering the load resistance below 4 ohms. The Livewire will control the variable load resistance from the Hall Effect sensors measuring the generator rotational speed. The scope of controls and variable load resistance are outside the scope of this paper, which used fixed load resistance for 3-wheel Power Take-off prototype.

2.5– Finite Element Analysis of the Hinging Mechanism

Finite element analysis studies were run on iterations of the acetal pieces of the Livewire nicknamed “bones’ to build a design that can deflect under high wire tensions. The Power Take-off relies on 4 acetal beams, the bones, which squeeze the generator and idler sheaves to the wire. The length and deflection of the bones determine the normal force of the generator wheel on the wire because they push the wheel between the sheaves. They have a smooth profile and expand at the connection holes to prevent stress concentrations. The dry test determined that the prototype bones were not rigid enough under normal operating conditions. When 50 kilograms were hung from the wire, the bones next to the wheel would bend outward, and bones on the opposite side would bend inward. The wire induced a moment around the near bones, twisting the frame away from the wire as shown by the figure below (Fig. 20)**.**

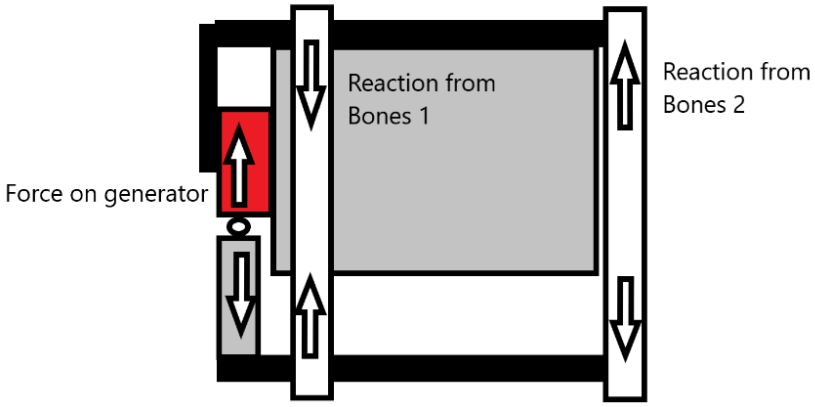

Figure 20: Power Take-off free body diagram from above used to estimate the forces and moments on the bones from the mooring wire.

The bones need to have negligible deflection at normal wire tensions but should deflect to a straight wire path under extreme conditions without failing. The fraction of the wire’s tension that pushes against the 3-wheel design decreases as the bones deflect outward and the wire offset angle decreases. At a straight wire path, the force on the generator is from bone spring and is unaffected by additional wire tension. In the current design, the wire is offset by 0.925”. Autodesk

Fusion 360 simulated forces which stretched the bones by 0.925” in the x-direction. The simulations were performed on the same CAD file that was uploaded to the routing table, and yield strength of acetal in Fusion matched the Delrin acetal from McMaster. The FEA studies below illustrate where the first design only had a safety factor of 0.29 when deflected .925” lengthwise (Fig 21).

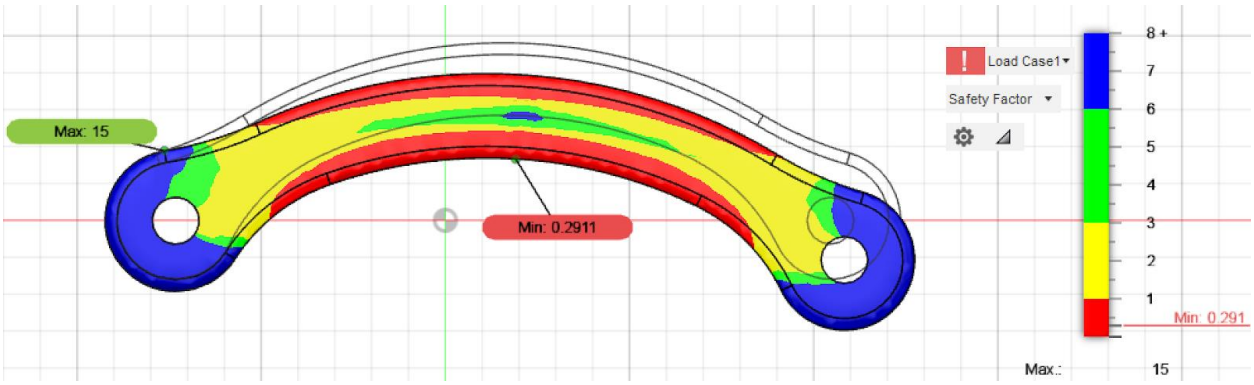

Figure 21: Initial bone shape static safety factor from FEA simulation of the Power Take-off with a straight wire path. The bones are deflected by .925” lengthwise between the connection points.

The current design shown below are stiff semi-circle beam springs that only achieved a safety factor of 0.8 for a deflection of 0.925” (Fig. 22). The 4.25” tall and 1.2” wide semicircle cut out of 1” thick acetal proved to be an effective bone shape for strength under normal loads around 113N, the force from 50kg of bottom weight. The extra width and thickness also help oppose the moment from the connecting rods around the bones. Increasing the width made this design less bendable, but the shape was too thick. The HDPE spine needed to be cut half as wide to fit the 1" thick bones 1 in the frame.

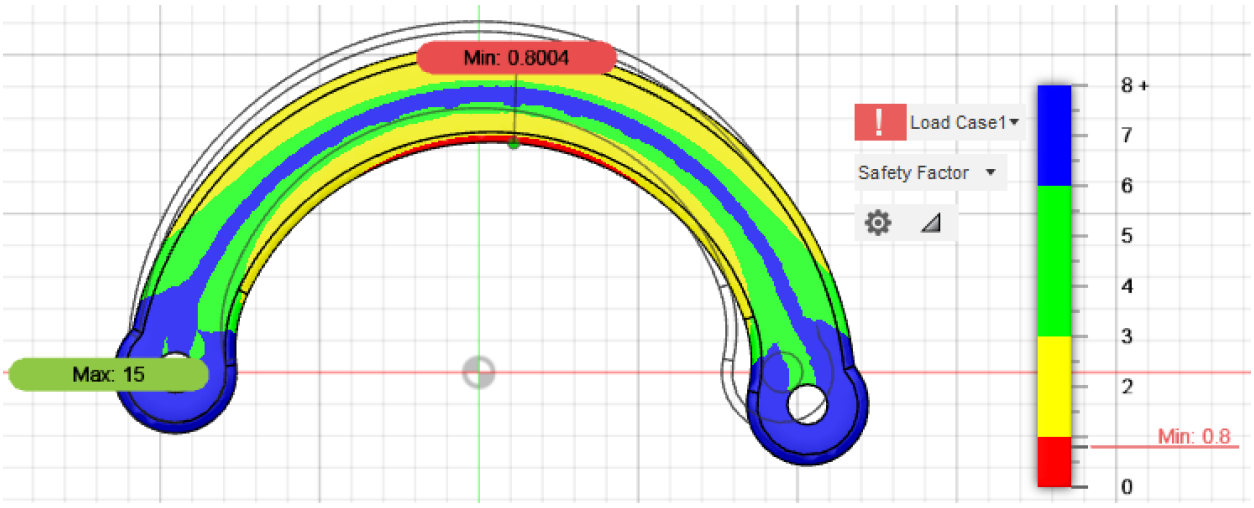

Figure 22: Improved bone shape safety factor from the same static FEA simulation as Fig. 21.

While these bones functioned as needed for the prototype better than the first pieces, they failed in three ways. The bones are too wide for the current frame, they did not reach a high enough safety factor for extreme conditions, and the force required to bend them 0.925” is greater than the 725 N rated internal bearing. The failures were due manufacturing the bones for profiler tests before correcting from FEA results and bearing calculations. The pool test concluded that the dimension of the bones needed to be adjusted to better grip the wire by further offsetting the wire from the vertical. The next bones should be designed for a Power Take-off with a larger wire offset angle, a higher safety factor, and a narrower profile.

CHAPTER 3: The Pool Test

3.1– Preparations for Submerged Tests

The system was fully waterproofed in preparation for the pool test. The generator was potted with epoxy and its cables were cut and re-wired with 6-pin adapters to run into the pressure case. Each of the three cables were cut, their individual wires soldered, and surrounded by shrink wrap, putty, and tape. The cables ran from the generator into the pressure case. An outgoing cable from the pressure case ran 40 feet to a bench setup to measure the voltage and control the circuit. Waveform logger software to recorded voltage across the load resistor and powered the relay to switch the load resistor on or off. The pressure case setup was tested before moving to the pool to by submerging it without the electronics to test the seals with a chalk line around the inside. The electronic included the 4.3-ohm load resistor, a relay switch, an AC to DC rectifier, and a capacitor as a low pass filter (Fig 23). The base plate of the circuit was a ¼" aluminum plate to act as a heat sink because the resistor would heat up in the bench tests. When the relay was powered with a 3-10V DC source, the circuit closed, and the resistor loaded. The closed relay allowed the Livewire to generate electricity when spun by the mooring wire.

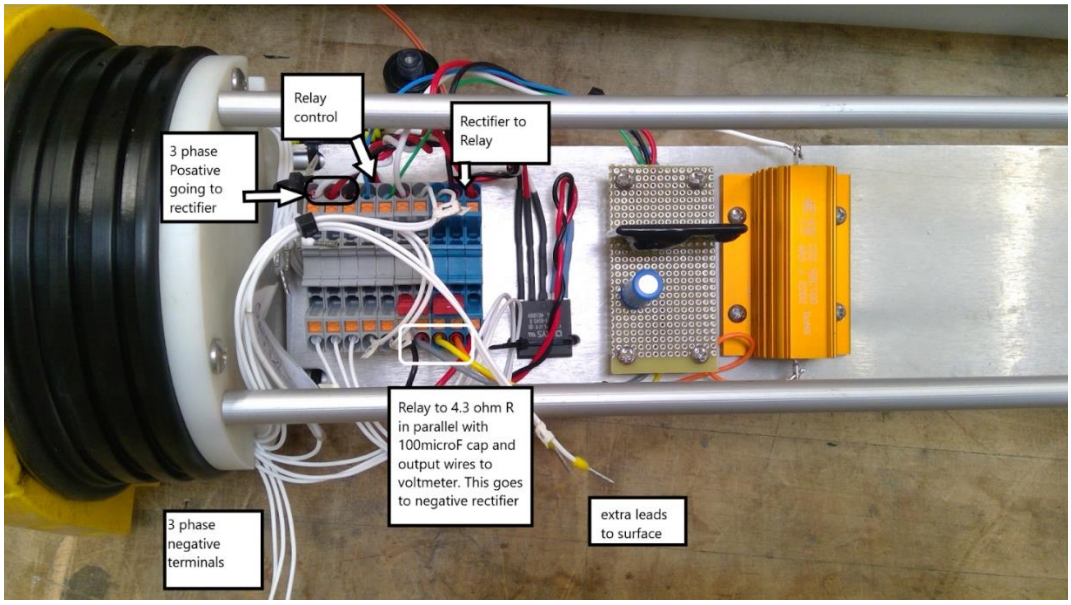

Figure 23: Photograph of the pressure case circuit with din-rail connectors, an AC-DC rectifier, relay switch, capacitor, and load resistor (left to right) mounted on an aluminum heat sink.

3.2– The Bench Test

The submersible Livewire was set up horizontally on the bench and tensioned wires were pulled through it to test the circuitry and Waveform logger graphs. The Livewire was clamped down, and the wire connected to a 23 kg weight. A rope connected the wire to the weight on the other side of a block mounted in a vice, giving about 2 feet of distance. Waveform software recorded voltage over the load resistor as the wire was pulled slowly through the profiler. The test was repeated with faster oscillations of a 23 kg bottom weight and with slow oscillations of a 46 kg weight. Power was calculated from the voltage over the load resistor and averaged over several wave cycles, peaking at 3-4 W. During the test, the block stopped rotating due to the pressure of the vice, which increased the tension when raising the weight and decreased it when lowering. The difference in tension can be seen in the mismatched power peaks (Fig. 25). Once the system worked as intended, it was brought to the Scripps test pool for a submerged test.

3.3 – The Pool Test Methods

At the Scripps Pool, a 35ft section of mooring wire was weighted with 54.3 kilograms of lead and lowered to the 15 ft shallow end of the pool via the crane. Then the Livewire was picked up with a second line to the crane, and the slack mooring wire was placed in the profiler's roller guides and across the three wheels. Then the crane was further raised off the shallow end, tensioning the wire, and placed at the bottom of the pool. Once on the bottom, the wire was tied to a rope that ran up through a block suspended by the crane and down to a counterweight on the pool bridge equal to the bottom weight. At this point the first line used to pick up the wire was disconnected, leaving the wire only connected across the pulley. There remained a slack safety line from the Livewire over the hook and tied off in case it sank. When the crane was raised, it picked up the bottom weight and the counterweight leaving a free hanging system that could be moved by hand (Fig. 24). The Livewire had a long waterproof cable that ran from the pressure case to a bench set-up. The cable had the relay switch controls and wires to measure the voltage across the 4.3-ohm load resistor.

Figure 24: Photograph of the Keck Pool test courtesy of Mai Bui with a very positively ballasted Livewire.

When the relay wires were connected to a 6V battery, the circuit would close, and the Livewire would generate power and increase load torque. When the relay disconnected, there was

no voltage across the resistor or load torque. To recreate a camming motion downwards, one person raised and lowered the wire while a second person turned the switch on for each lowering stroke. 2-way camming was attempted at neutral buoyancy, and 1-way camming and floating ascent was attempted at a slight positive buoyancy. The Livewire was initially ballasted with 12 blocks of foam, which were slowly removed until the system was as close to neutrally buoyant as possible. With the current set-up the system only needed 5 pieces to become neutrally buoyant.

3.4 – The Pool Test Results

The pool test only generated an average power of 0.1 watt, while the dry test generated an average of 0.5 and 0.9 watts depending on wire tension (Fig. 25). These numbers are far below the values that the generator can produce (> 30 W) when driven by a motor (Fig 16), demonstrating that the "omega drive" prototype was not yet fully optimized. The peak power can be compared to the power curve, but an average over many wave cycles is a realistic power output when profiling. The power graph below shows that peak generator power was limited by the gripping force on the wire. Doubling the wire tension from 23 kgf to 46 kgf nearly doubled the power from 0.55 to 0.91 watts, while doubling the wave frequency only increased the power from 0.55 to 0.83 W. The large impact of wire tension suggests that current 3-wheel design needs a better grip on the wire. Video recordings of the dry testing set-up confirm that the generator wheel was slipping on the wire while still rolling. In the pool test, the Livewire generated 0.1 W (average) with a peak of 1 W, presumably due to the wet C.O.F., lost efficiency from moving in the water column, and rolling friction, and other frictional losses in the omega drive sheave system. Power was limited by sliding friction when the profiler was clamped down, but in the pool test power was also limited by inertia and drag in the water. Even with perfect grip, rolling resistance reduced the load torque that the generator could receive from the drag and inertia of the profiler.

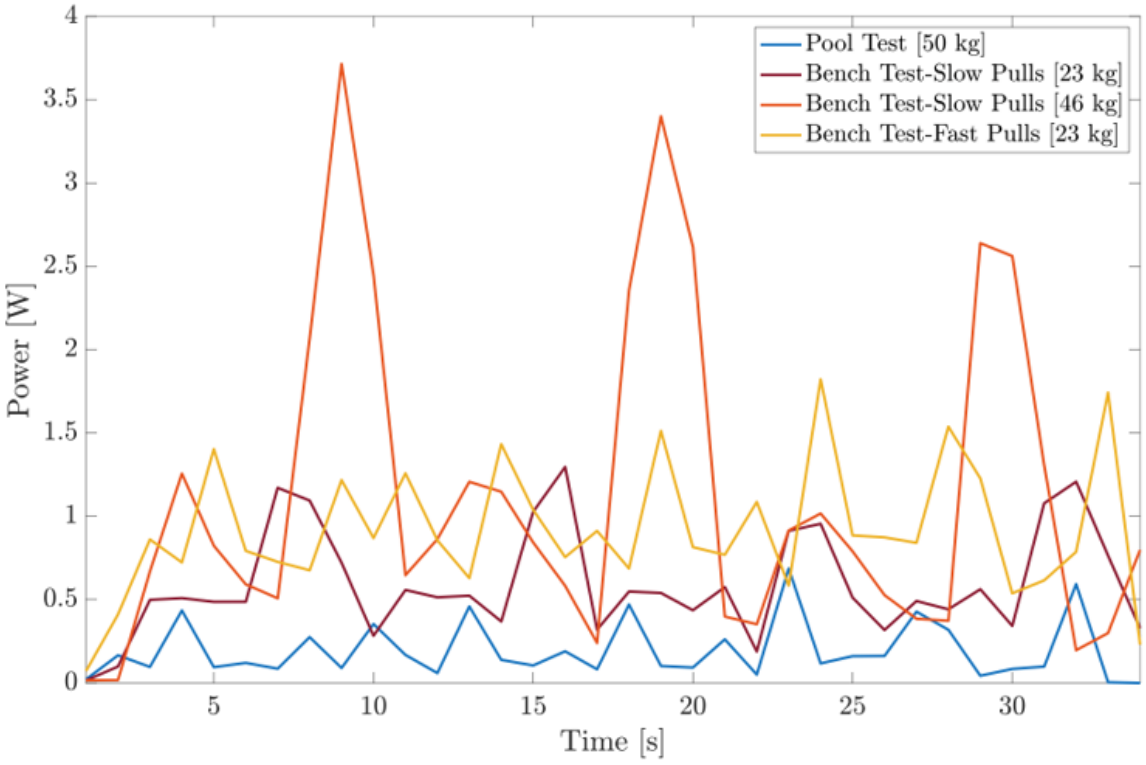

Figure 25: Generated Power (W) over Time (s) for the Livewire bench and pool tests. Power was found from the voltage across the 4.3-ohm load resistor using a Waveform Data Logger.

The current Livewire does not travel up and down the wire as intended. The mooring wire slips through the loaded clutch in fast waves, and the unloaded clutch cannot decouple from the wire motion in slow waves. Travel up and down the wire was achieved, but only changing the speed of the heave between the up and down stroke. The Livewire frame needs to be more neutrally buoyant than a Wirewalker and increase its grip without increasing rolling resistance. When camming down, a Wirewalker easily decouples when the rollers separate at the top of the v-groove cam. Livewire is worse at decoupling because the generator's rotational inertia and various forms of friction pull the profiler up with the upstroke of a wave, in addition to buoyancy. The compounding effects of internal friction and buoyancy made a positively ballasted Livewire very poor at camming downwards and removed the possibility of a Wirewalker-like ascent. The profiler

needs better grip to generate power and stay coupled, and to reduce the rolling resistance to decouple in small waves.

A locked sheave could have been a significant source of the rolling friction, but the issue was unnoticed until removal from the pool. A sheave bent between the acetal plates at some point during or right after the experiment due to the imbalanced Livewire being held vertically by the wire tension. The offset weight of the generator misaligned forces onto the sheave and compromised the pocket machined to press-fit the bearing. In the next pool tests, sheaves should be a stronger material and better constrained. Slippage should be quantified using a combination of Hall effect measurements and an IMU to compare the rotation of the generator and vertical acceleration of the platform.

3.5 – Pool Test Analysis

The current prototype can generate electricity but does not profile. In light waves, the rolling friction and generator inertia overpower the drag term causing the profiler to stay in phase with the wave motion. In heavy waves, the profiler is slipping regardless of if the generator torque is high or low.

The profiler will generate more power with a better fictional gripping force on the wire as seen by the 46 kg bench test (Fig. 25). Non-dimensionalizing gripping friction by dividing wire tension (F_{fr}^{*}) creates a useful parameter for describing a 3-wheel design that efficiently generates power over a wide range of conditions. High F_{fr}^{*}values correspond to low losses from the wire forces on the wheel and sheaves, making it easier to decouple the profiler from the wave motion. The Capstan equation shows the effects from increasing the coefficient of friction and contact angles on F_{fr}^{*} (Fig. 26).

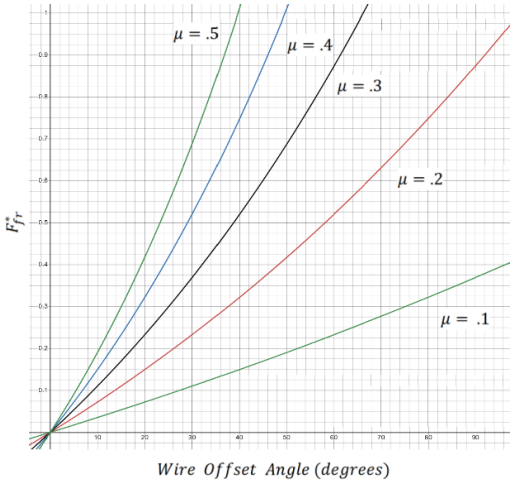

Figure 26: Frictional gripping force as a fraction of the wire tension versus wire offset angle relative to vertical with COF values from 0.1-0.5 by plotting the Capstan equation.

The wire can be wrapped further around the wheel to increase the holding force as per the Capstan equation. To do this, the acetal plates holding the sheaves should be re-made to increase the contact angle by further offsetting the wire from the vertical. Another way to increase grip on the wire is with a higher coefficient of friction. The flat 95a polyurethane surface of the generator wheel could be replaced by a textured metal v-groove like Harken self-tailing winches. The HDPE sheaves need to be replaced with a stronger material and additional clearance from the side plates. A locked sheave could have had the largest impact on 1-way travel, but repeated tests could confirm why the profiler did not decouple when the generator was unloaded.

If the Livewire can get a grip on the wire, but cannot decouple, then the drag coefficient should be increased. Drag could be increased to encourage decoupling from the wave motion to overcome the frictional losses and inertia from the wire on the profiler. This tactic can be seen in the very first Wirewalkers, where drag from a square bottom plate helps the profiler stay in position when the cam tries to disengage on the upstroke of a wave. The frictional gripping force must be greatly improved before using additional drag like fixed or folding wings to overcome rolling friction.

CONCLUSION

Livewire generates power from surface waves by using the relative motion between the profiler and the mooring wire to spin a generator. The Livewire's cable drive system, or clutch, relies on the grip of a single wheel on the wire while minimizing frictional losses to cam in one direction and efficiently generate power. In this paper, the design process of a 3-wheel hinging clutch and results from a pool test are presented to guide further development of the Livewire. The wet coefficient of the 95a polyurethane generator wheel, 0.17, was too low for a pinch roller design because the normal forces required to grip the wire created significant rolling friction and inelastic deflection on the wheels. The ideal load resistance for the generator is 4.3 ohms from a power curve test. A 3-wheel hinging clutch is presented that distributes pressure around a section of the wheel by pushing the wheel against the wire between two sheaves. The design benefits from increased frictional holding force from the Capstan equation, but most experimental results confirmed that the wire was still slipping. The pool test confirmed that this 3-wheel design did not provide enough friction for one way motion on the wire. The Livewire only generated 0.1 W (average) and 1 W (peak) in the water compared to the 0.5 to 0.9 (average) and 3-4 W peak during testing in air because the omega drive system slipped at high instances of acceleration and then was dragged with the wire from internal friction on the wheel and sheaves. Both tests of the power take off showed that the system caused significant loss, given the demonstrated generation capacity of the motor/generator with optimal loading. Finally, changes to the dimensions, materials, and surfaces are recommended for better performance in the future.

APPENDIX

A 1: Inelastic deformation of the 95a polyurethane wheels in the pinch roller from friction tests. The deformation introduced error in the COF results since the normal force calculation assumed only elastic deformation. The effect caused the wire to slip at lower tensions between tests.

Table 2: Complete list of variable definitions

Variable	Symbol	SI Units
Generator wheel radius	R	m
Generator constant	k_g	V-s
Rot. velocity of gen.	ϖ_g	Rad/s
Rot. acceleration of gen.	α_g	Rad/s^2
Moment of inertia of rotor	I_g	Kg-m^2
Motor/gen. input voltage	V_{in}	V
Sliding velocity	v	m/s
Relaxation time	τ	s^{-1}
Load torque	T_{load}	Nm
Rolling friction	$F_{R,fr}$	N
Static/Sliding Friction	$F_{s,fr}$	N
Profiler-wire force	F_w	N
Normal force on wheel	N	N
Coefficient of rolling friction	$\mu_{rolling}$	-
Coefficient of sliding friction	μ_s	-
Wave frequency	σ	s^{-1}
Wave Amplitude	A	m
Vertical wave velocity	w_{wave}	m/s
Relative velocity of the wire to the profiler	w_w	m/s
Effective Youngs Modulus	E^*	Pa
Effective Radius	$\tilde{R}$	m
Corrected bottom weight mass	m_w^*	kg
Wire offset angle	φ	rad
Dim-less Friction Force	F_{fr}^*	-

REFERENCES

Austin, Hughs. 2019. *Electric Motors and Drives: Fundamentals, Types and Applications 5th Edition*. 5th ed. Newnes.

Harrison, Mark. 2013. “Physical Collisions and the Maximum Power Theorem: An Analogy between Mechanical and Electrical Situations.” *Physics Education* 48 (2): 207–11. https://doi.org/10.1088/0031-9120/48/2/207.

Kundu, Pijush. 2015. *Fluid Mechanics*. Vol. 6th. Academic Press. https://www.elsevier.com/books/fluid-mechanics/kundu/978-0-12-405935-1.

Le Boyer, Arnaud. 2022. Personal Communications.

MODLab. 2021. “Hertz Contact Mechanics of Live Wire Drive Cable.”

Pinkel, R., M. A. Goldin, J. A. Smith, O. M. Sun, A. A. Aja, M. N. Bui, and T. Hughen. 2011. “The Wirewalker: A Vertically Profiling Instrument Carrier Powered by Ocean Waves.” *Journal of Atmospheric and Oceanic Technology* 28 (3): 426–35. https://doi.org/10.1175/2010JTECHO805.1.

Popov, Valentin L. 2017. *Contact Mechanics and Friction, Physical Principles and Applications*. Vol. 2. Springer.

Popov, Valentin L., Markus Heß, and Emanuel Willert. 2019. *Handbook of Contact Mechanics: Exact Solutions of Axisymmetric Contact Problems*. Berlin, Heidelberg: Springer Berlin Heidelberg. https://doi.org/10.1007/978-3-662-58709-6.

“The Wirewalker: How It Works.” n.d. Del Mar Oceanographic. Accessed November 28, 2022. https://www.delmarocean.com/ww-how-it-works.